

---

## Recent GRBs observed with the 1.23m CAHA telescope and the status of its upgrade

Javier Gorosabel<sup>1</sup>, Petr Kubánek<sup>1,2</sup>, Martin Jelínek<sup>1</sup>, Alberto J. Castro-Tirado<sup>1</sup>, Antonio de Ugarte Postigo<sup>3</sup>, Sebastián Castillo Carrión<sup>4</sup>, Sergey Guziy<sup>1</sup>, Ronan Cunniffe<sup>1</sup>, Matilde Fernández<sup>1</sup>, Nuria Huélamo<sup>5</sup>, Víctor Terrón<sup>1</sup>, Nicolás Morales<sup>1</sup>, José Luis Ortiz<sup>1</sup>, Stefano Mottola<sup>6</sup>, and Uri Carsenty<sup>6</sup>

<sup>1</sup> Instituto de Astrofísica de Andalucía (IAA-CSIC), 18008 Granada, Spain.

<sup>2</sup> Imaging Processing Laboratory (IPL), Universidad de Valencia, Valencia, Spain.

<sup>3</sup> INAF/Brera Astronomical Observatory, Via Bianchi 46, 23807, Merate(LC), Italy.

<sup>4</sup> Universidad de Málaga, Málaga, Spain.

<sup>5</sup> LAEX-CAB (INTA-CSIC); LAEFF, PO Box 78, 28691 Villanueva de la Cañada, Madrid, Spain.

<sup>6</sup> Institute of Planetary Research, DLR, Berlin, Germany.

We report on optical observations of Gamma-Ray Bursts (GRBs) followed up by our collaboration with the 1.23m telescope located at the Calar Alto observatory. The 1.23m telescope is an old facility, currently undergoing upgrades to enable fully autonomous response to GRB alerts. We discuss the current status of the control system upgrade of the 1.23m telescope. The upgrade is being done by our group<sup>7</sup> based on the Remote Telescope System, 2nd Version (RTS2), which controls the available instruments and interacts with the EPICS database of Calar Alto. Currently the telescope can run fully autonomously or under observer supervision using RTS2. The fast reaction response mode for GRB reaction (typically with response times below 3 minutes from the GRB onset) still needs some development and testing. The telescope is usually operated in legacy interactive mode, with periods of supervised autonomous runs under RTS2. We show the preliminary results of several GRBs followed up with observer intervention during the testing phase of the 1.23m control software upgrade.

---

<sup>7</sup> Our group is called ARAE (Robotic Astronomy & High-Energy Astrophysics) and is based on members of IAA (Instituto de Astrofísica de Andalucía). Currently the ARAE group is responsible to develop the BOOTES network of robotic telescopes [14]. See <http://www.iaa.es/arae/> and <http://www.iaa.es/bootes/index.php> for more details.



**Fig. 1.** View of the Calar Alto observatory. The picture shows the five telescopes of Calar Alto and the staff building (lower-right corner). The arrow shows the localization of the 1.23m telescope.

## 1 Introduction

The 1.23m telescope is at the German-Spanish observatory of Calar Alto (CAHA) in the province of Almería, South-East of Spain. The observatory's altitude (2168 m), mean seeing (0.9''; see [23]) and a large fraction (65%) of clear nights, make Calar Alto one of the most competitive observatories in Europe in the optical and near-infrared bands. The observatory harbours five telescopes, but only three are currently operative: the 1.23m, 2.2m and 3.5m telescopes. Fig. 1 shows a view of the Calar Alto observatory. The arrow indicates the position of the 1.23m telescope.

The 1.23m telescope is a Ritchey-Crétien telescope built in 1975 by Carl Zeiss. The focal ratio of the telescope is  $f/8$  with a total field of view of  $90'$  and a focal plane scale of  $\sim 20.9''/\text{mm}$ . The aberration free field of view is limited to  $\sim 15'$ . The German mount of the telescope is driven by a mechanical and hydraulic system renovated in 2008 by the observatory staff. Fig. 2 shows a drawing and a picture of the of 1.23m CAHA telescope.

Two instruments are available for the 1.23m, the MAGIC near-infrared camera and the 2kx2k SITE#2b optical CCD. Currently, most of the time ( $\sim 95\%$ ) only the optical CCD is used, as the MAGIC camera, one of the

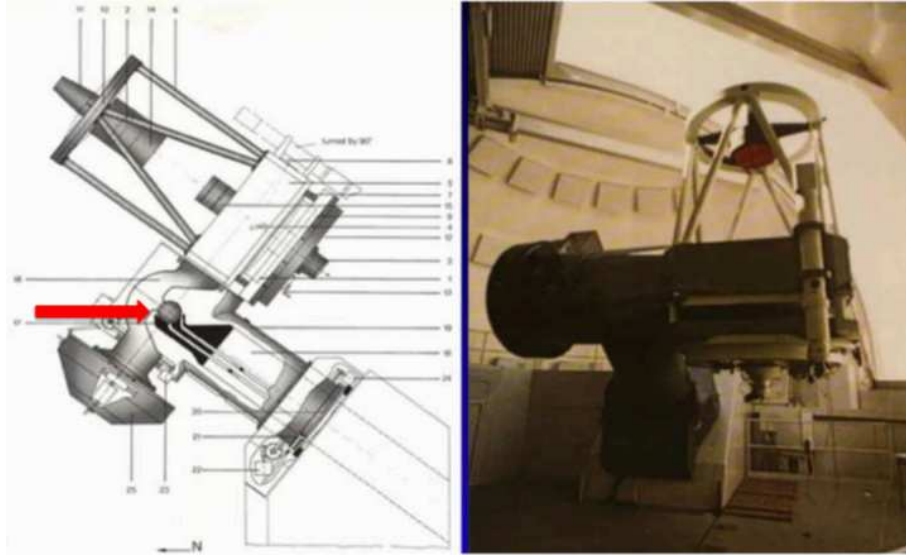


**Fig. 2.** The 1.23m telescope of Calar Alto. *Left panel:* the drawing shows the mechanics and the hydraulic system of the 1.23m telescope of Calar Alto. One of the mechanical peculiarities of the telescope is the presence of a steel sphere (indicated by a red arrow) which, by means of a high-pressure hydraulic system, supports all the weight of the telescope. *Right panel:* Picture of the 1.23m inside the dome. As seen the instrumentation is always located in the Cassegrain focus. Note the German mount of the telescope.

first near-infrared cameras ever built, was superseded by modern instruments on larger telescopes. In addition to the offering of the MAGIC near-infrared camera, CAHA is considering the possibility of installing visitor instruments on the 1.23m telescope.

The field of view of the optical CCD camera is  $17' \times 17'$  with a pixel size of  $24 \mu\text{m}$ . That translates to a pixel scale of  $0.5''$  per pixel. The read-out time of the whole chip in  $1 \times 1$  binning mode is very long, close to 4 minutes. For this reason rapid follow-up observations of transients like Gamma-Ray Bursts (GRBs) are usually carried out trimming the window and/or binning the CCD by  $2 \times 2$  pixels. Using this technique, the readout time is usually kept below one minute.

The CCD chip is refrigerated using liquid nitrogen, which makes dark current negligible, fewer than 2 electrons per hour. The read-out noise is also low, about 7 electrons. However, the chip has several bad columns which RTS2 (see next Section and [16]) must avoid at the time of a GRB alert (see the vertical lines on the image of GRB 090628, Fig. 7). The optical camera is equipped with a *BVRI* filter wheel. A Wollaston prism can be also mounted in the filter wheel, which makes the 1.23m telescope suitable also for polarimetric studies.



**Fig. 3.** The MAGIC near-infrared and optical CCD cameras of the 1.23m telescope, both in the Cassegrain focus of the telescope. *Left panel:* MAGIC near-infrared camera. The MAGIC detector is a 256x256 pixel HgCdTe array, providing a field of view of 4'x4'. The filter wheel of MAGIC allows *JHK* broad-band imaging. The instrument is only mounted by special request, so is not usually available. *Right panel:* Optical CCD camera running on the 1.23m telescope of Calar Alto. The optical CCD camera is based on a 2kx2k SITE#2b chip. The green tube is the dewar and the white box is the electronic system associated to the camera. The filter wheel is located in the black flange just on the detector dewar.

## 2 Upgrading the 1.23m control software with RTS2

A call for proposals was issued by CAHA in 2008 for the use of the 1.23m telescope over 4 years. Six teams obtained observing time, having the following scientific drivers: Solar System bodies, Binary stars, Transits of exoplanets, T Tauri stars, and GRBs. The 1.23m is also scheduled for public outreach purposes, usually associated to high-schools.

The ARAE (Robotic Astronomy & High-Energy Astrophysics) group of IAA<sup>8</sup> agreed to contribute to CAHA by providing the control system of the 1.23m telescope. The ARAE group was granted 26 GRB triggers per year with an average duration of 0.5 nights per trigger. The upgrade of the telescope and its instrument control system is currently being carried out based on RTS2 (see [16] and references therein). One of the key requirements of the upgrade is to keep the existing telescope software and hardware untouched. The system must remain operational every night throughout the upgrade.

As none of the telescope instruments, nor their control electronics and software was developed by our group, we are kept away from the complex details of their construction and internal operation. As described later, we exclusively communicate with the control interfaces of the existing software.

The existing control system is an adapted version of that currently used by the 3.5m Calar Alto telescope. It allows the observer to control the instruments through graphical user interface (GUI) programs running on two

<sup>8</sup> Instituto de Astrofísica de Andalucía, partner in the CAHA operations.

main observatory computers - one for the telescope control, the other for the camera. The observer is responsible for preparing the observing plan, opening and closing of the dome, taking care of executing exposures, inspecting images for good pointing and their quality, and synchronizing the telescope and the filter wheel movements with the CCD exposures. The major drawbacks of this approach are obvious: the observer spends most of the night working hard to get the data and keep the system running, the system is prone to human errors when the observer is tired. Moreover, the observing logs are either hard to extract from the technical log or are not created by the system at all, and the interruption of the observation to react on a quickly evolving target of opportunity requires observer presence and attention.

In contrast, RTS2 was designed to create an autonomous observatory environment. The observer is allowed to interact with the system, and at worst case to take full manual control. The system is able to guide the observatory through the night, taking care of closing and opening the dome, acquiring sky flats, darks, and last, but not least, keeping detailed logs of the images acquired, judging pointing accuracy and producing preliminary results.

RTS2 device drivers are responsible for handling any errors that occur during their operation. If possible, the device is reset, and another attempt to get it operating is made. The RTS2 *rts2-xmlrpcd* component is responsible for communicating the errors to the users and custom scripts, which allows for the execution of more complicated scenarios. One of the core principles is to avoid restarting drivers that have failed. If the driver produces a core dump, that is safely removed from the system and it is up to the observer to restart it. This feature also allows RTS2 to be quite flexible – for example a configuration without any telescope, just with a camera and other instrumentation, can be made without changing a single line of code. More information on handling the errors and other related issues is provided in [18].

The autonomous capabilities of the RTS2 system resides in a generic layer, with underlying hardware-specific drivers and communication via the TCP/IP network stack. So in an ideal world, once the provided skeleton drivers are used to write low level RTS2 drivers for the hardware, every telescope can be made fully autonomous. To our knowledge, this is a big step forward from the traditional, incremental way of how observatory control software has been developed. Instead of being written primarily as a set of controls for the hardware, with some subsequent autopilot features, RTS2 was designed from the start to provide autonomous capabilities. Secondly RTS2 also provides a way for the observer to interact directly with the hardware.

## 2.1 Current state of the upgrade

Development of the first version of the RTS2 drivers was a question of a few days (and nights), since the RTS2 drivers were being written by the main author of RTS2 (with the assistance of the CAHA staff). The major obstacle which we had to face was running RTS2 on an old Solaris operating system,

which is used to run the 1.23m control computers. As RTS2 was written in quite portable C++ on Linux, and using GNU Autotools<sup>9</sup> for build control, the porting process involved changing a few unavailable functions<sup>10</sup>. The system is now able to operate the same as any other observatory using RTS2.

The remaining obstacle is the lack of a natural incorporation of the auto-guider in the RTS2 environment. This fact prevents us from taking images with long exposure times. Tests performed with the 1.23m showed that exposures longer than 300s produce elongated Point-Spread-Functions (PSFs), especially under sub-arc-second seeing conditions. The guider is an old instrument, with a quite complicated interface, without any autonomous capabilities. Thus, some time will be needed before we will be able to perform observations with the guider smoothly integrated in RTS2.

Currently the 1.23m is able to respond to GRB alerts generated by the GRB Coordinates Network (GCN). The maximum slew time of the 1.23m telescope is 4 minutes for the most unfavourable move. Usually the response time is below 3 minutes. The response time is limited by the speed of the current engines/mechanics moving the dome and the telescope. Given that the existing telescope/dome mechanical parts are strong and reliable, CAHA does not plan to renew them, so we do expect to overcome the slew-time limitation in the near future. The RTS2 Gamma-Ray Burst Daemon (*rts2-grbd*) of the 1.23m is continuously linked via TCP/IP network socket to the GCN server at Goddard Space Flight Center (GSFC). In order to react to GCN alerts, it was necessary to accommodate the GCN connection in the CAHA firewall. Fig. 4 shows a working scheme of the 1.23m response mode to GCN alerts under RTS2.

When a high-energy satellite (usually the *Swift* mission with its BAT[1] detector) localizes a GRB, the position is dumped in a few seconds from the GRB occurrence to ground-tracking stations and distributed by the GCN to its subscribers. In our case the GCN packet reaches the CAHA *rts2-grbd* server. Then the ongoing observations are interrupted and the 1.23m is pointed towards the GRB position in order to start a series of short exposures (usually with the CCD windowed and binned in order to save read-out time). Interrupting an observing run is a standard mechanism in RTS2 (see details in [18]). The interruption can either be hard, which interrupts the current exposure, or soft, which waits the current exposure to finish. The rules governing this choice will be decided by the observers once the system is fully operational.

The RTS2 control system stores most of the data in a *Postgresql* database<sup>11</sup>. It includes tools for retrieving and manipulating information from the database. New targets can be entered through command line tools, autonomously from various triggering systems, or from the RTS2 Web interface.

<sup>9</sup> GNU Autotools web site, <http://www.gnu.org/software/autotools>

<sup>10</sup> and renaming the variables called "sun" ("sun" is a defined symbol on Solaris systems).

<sup>11</sup> Postgresql web site, <http://www.postgresql.org>

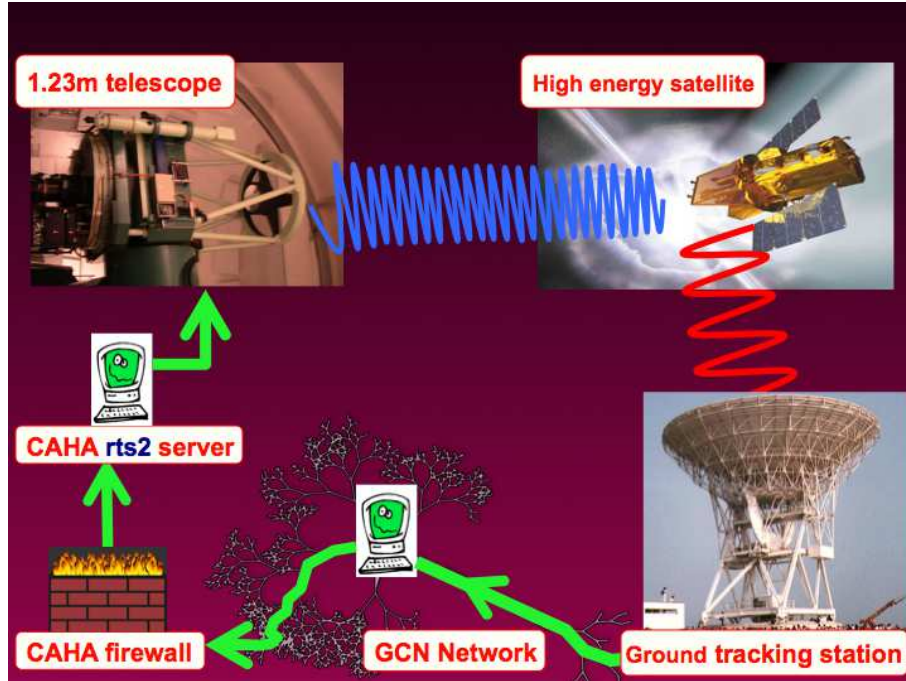


**Fig. 4.** Flow diagram of the GCN network and the response mode of the 1.23m telescope. The whole process can take up to 4 minutes, depending on the position of the GRB on sky. The time needed to receive the coordinates from the high-energy satellite in the RTS2 server takes just a few seconds (usually less than 15 seconds). Currently most of the delay is due to the slow pointing of the 1.23m, which could take up to 4 minutes in the worst case.

The system has a powerful internal scripting engine, which enables users to define the observing strategy. By tracking devices states, the system handles synchronization among instruments, so the user does not have to know the details of the execution of the underlying observation. Scripting enables the user to specify all image parameters, dithering strategy, selected filters, and much more. For example the following script runs observations in  $I$ -band, based on a series of 9 dithered images with a exposure time (per frame) of 240 seconds, with a 1x1 CCD binning and trimming the CCD to a sub-window of 500x400 pixels [ $x1=600$ ,  $x2=1100$ ,  $y1=300$ ,  $y2=700$ ]:

```
FW0.filter=I READT=(600,500,300,400) binning=1 E 240
T0.WOFFS=(-72s,+36s)
for 3 { for 3 { E 240 T0.woffs+=(16s,-54s) } T0.woffs+=(0,+3m) }
```

Note that the syntax for the sub-window in the above example is ( $x1$ ,  $x2-x1$ ,  $y1$ ,  $y2-y1$ ). We have incorporated in RTS2 a call to the automatic

astrometric calibration package described in [7]. This "on-the-fly" astrometric calibration corrects the telescope pointing, so the object can be placed on the desired (x,y) coordinates of the detector. The optical distortion on the CCD is negligible (less than one tenth of a pixel), so we decided to make a simple (and hence fast) fit considering a rotation term and a center field shift. The astrometric calibration is done on every frame. Polynomial fit is not used. The typical astrometric error (using  $\sim 20$  stars) is below  $0.5''$ , good enough to correct the 1.23m pointing. The typical standard deviation in the inferred rotation angle is  $\sim 0.1$  degrees when  $\sim 20$  field stars are used in the fit. The success rate of the "on-the-fly" calibration is above 95%. The astrometric calibration of the remaining images is done manually afterwards.

In the near future we plan to provide also a rough photometric calibration based on the USNO-B catalogue [22]. Simultaneously to the telescope triggering an e-mail is sent to the 1.23m users to warn them on the occurrence of the GRB. Additionally the GCN alert triggers the creation of an e-mail and a SMS for the ARAE group with relevant information of the GRB (coordinates, Galactic reddening, finding chart, elevation curves, and other information). Please see [4] for more details about this system.

Further improvements on this status are likely doable, so we feel confident that, under the current limitations (for instance the telescope slew speed), we could reduce the GRB response times. This might allow us to detect the prompt optical emission associated to the gamma-ray event.

Another potential upgrade of the 1.23m telescope could be the incorporation of MAGIC in RTS2. Rapid response observations with MAGIC would make the 1.23m telescope very competitive in the GRB field. Currently this is beyond our scopes (and also beyond the CAHA man-power maintenance capabilities), but we do not discard it since the flexibility of RTS2 to accommodate new devices would allow us to integrate MAGIC (and new possible visitor instruments) quickly.

## 2.2 Integration of the legacy interfaces to RTS2

The following subsections provide descriptions of the legacy interfaces and their interaction with RTS2.

### Interaction of RTS2 with the Calar Alto EPICS

The individual operations of the CAHA telescopes are coordinated, and controlled, by the Experimental Physics and Industrial Control System (EPICS<sup>12</sup>). The task of EPICS is to provide access and control of all the CAHA telescopes, as well as data from the central weather station and from the seeing and extinction monitors. The seeing and extinction monitors are based on small aperture telescopes located in CAHA whose values are available through EPICS.

<sup>12</sup> EPICS web site, <http://www.aps.anl.gov/epics/index.php>

The 1.23m telescope mount, its focuser and the camera filter wheel are all fully controllable through EPICS. The legacy telescope interface accepts objects coordinates in the J2000 coordinate system, and handles all the required calculations internally, including precession, aberration, reflection and telescope pointing model offsets. Both the filter wheel and the focuser can be controlled through their own EPICS channels. Other devices in the 1.23m telescope system do not exist in the EPICS universe: the CCD detector, the auto-guider camera, the dome itself, and various auxiliary switches (for example the dome lights).

We use the information provided through EPICS to automate several tasks of the 1.23m. For instance, the meteorological information available from the EPICS is used to trigger the bad weather state, and hence to close the dome<sup>13</sup> and stop observations. Bad weather is also triggered when both other telescopes are closed - this is the rule imposed on the 1.23m operations by CAHA. For discussion on how the weather state voting is integrated into RTS2, including its fail-safe capabilities<sup>14</sup>, please see [18].

Yet another possible application lies in coordinating observations with the other Calar Alto telescopes. From the EPICS system, RTS2 can learn what the targets of the other telescopes are, whether they are in the RTS2 database, and depending on the target information can either start their monitoring or remove them from the list of targets which should be observed.

### CCD integration within RTS2

The optical CCD detector is connected to its own control computer. The control computer communicates with the control software, running on a master workstation, over the network. From the available C source code, we created a RTS2 device driver. All the major settings are supported, including binning and partial chip readout. The camera behaves as just another RTS2 supported CCD camera, visible in monitoring software and available for scripting.

### Guider camera and its integration in RTS2

The guider is built from a video camera with an image intensifier, fed from a pick-off mirror on a two-axis stage. This allows to place the guider image anywhere in the telescope field of view (FoV), thus eliminating the significant disadvantages of autoguiding-by-astrometry using the main camera: limited detector FoV, low gain and a requirement for short exposure times. The guider camera has its own control computer, which assumes the observer is sitting in

<sup>13</sup> Based on calculated Sun position through *libnova*, <http://libnova.sf.net>

<sup>14</sup> Network crashes and other failures (including the EPICS ones) are properly handled inside RTS2. A detailed description on how the weather voting system works is beyond the scope of this paper. We refer the reader to the extended discussion given in [18].

front of it (e.g. the video output is sent directly to the screen). Partial remote control has since been provided, in part by placing a web camera in front of the guiding screen.

We would like to improve this setup with a fully integrated RTS2 device, which would transparently provide automatic search for bright stars in the FoV, and guiding capabilities. In principle, RTS2 is able to do this, and some promising tests were already carried out on the other RTS2 controlled telescopes. Currently the biggest problem is to figure out how to communicate with the guider, and to implement a full auto-guiding loop.

### Dome control and other switches

As the dome is a critical component, its control is separate from the EPICS system (although dome status is reported to EPICS). In order to change the dome state, special commands must be run on the dome control computer. Similar commands are available to turn off and on dome lights, to control the telescope drives, the hydraulics, the tracking and the mirror cover. Those commands are fully interfaced in RTS2, so RTS2 is able to control all those switches.

## 3 Preliminary results

Although not fully autonomous, the 1.23m has already performed follow up optical observations of GRBs. None of the results below itemized were acquired by the automatic response mode of the RTS2 package, but some data were manually acquired by using RTS2 as the observing tool. Most of the data were taken by *in situ* observes, using the currently available GUI.

All the below listed GRBs showed X-ray afterglows which were localized by the XRT X-ray telescope on board *Swift* (see [2] for detailed information on the XRT instrument). So their X-ray afterglows were localized with uncertainties of only a few arc-seconds, making the corresponding optical studies much more efficient.

### *GRB 090313:*

The optical afterglow of this GRB [5] was observed with the 1.23m in the *R*-band during two consecutive nights one week after the gamma-ray event. The observations were accompanied with *K*-band observations carried out with the 3.5m telescope of Calar Alto equipped with Omega<sub>2000</sub>. The data of the afterglow are currently being analyzed and are part of an international monitoring which will be published in [21].

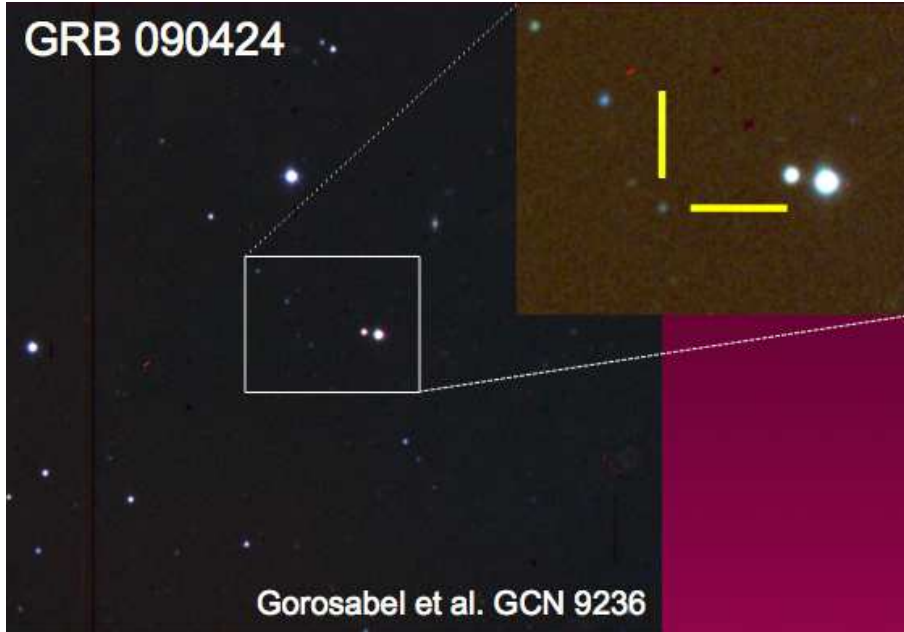


**Fig. 5.** The figure shows the optical afterglow of GRB 090424 as detected with the 1.23m CAHA telescope. The image has been created by combining *BVRI*-band images taken with the 2kx2k CCD camera currently in use. The upper right box shows a magnified picture of the afterglow region. The magnitude of the afterglow was  $R = 19.3$ . The mean observing epoch of the image is April 24.87 UT. North is up and East right. The field of view of the images is  $8' \times 8'$ .

*GRB 090424:*

We detected the afterglow of GRB 090424 [3] in *BVRI* on April 24.87 UT with a magnitude of  $R = 19.3 \pm 0.1$ . The preliminary results were reported in [9]. In the days following GRB 090424, a long term monitoring was performed in *R* and *I* bands in order to search for the underlying supernova. Fig. 5 shows a colored image constructed with the *BVRI* 1.23m images taken on April 24.87 UT. The final results have been included in [15].

*GRB 090621B:*

We detected the two afterglow candidates reported for this GRB [6] by Levan et al. and Galeev et al. [19, 8]. The observations were done in the *I*-band, 4.14 - 4.75 hours after the GRB. A deep second epoch observation is pending in order to search for photometric variability of the candidates. The preliminary results were reported in [10]. Fig. 6 shows both candidates.

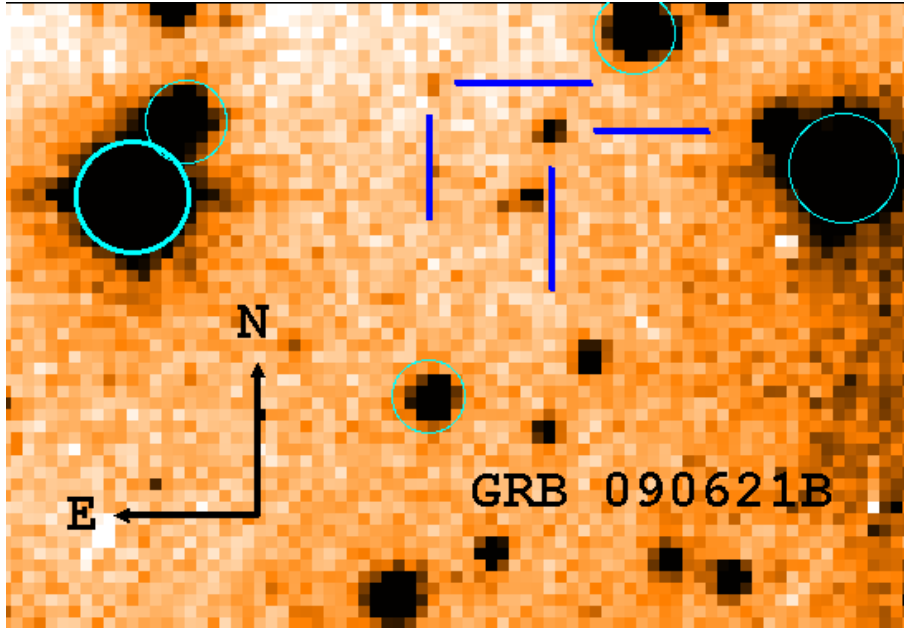


**Fig. 6.** The picture shows the co-added  $I$ -band image taken for GRB 090621B with the 1.23m telescope of Calar Alto. The faintest of the two objects (the most upper one indicated with tick-marks) represents the candidate reported in [19]. Approximately  $10''$  towards the South-West it is marked the candidate reported by [8], brighter than the one of [19]. The cyan circles shows the USNO-A2 catalogue stars used for the astrometric and photometric calibration. The field of view of the image is  $70'' \times 50''$ , with North up and East left.

*GRB 090628:*

$R$ -band observations of the XRT position [24] were carried out 1.43–3.20 hours after the gamma-ray event. No counterpart was found down to  $R = 22$  in the XRT error box. Simultaneous near-infrared observations would have been very helpful in order to discriminate the possible high-redshift nature of this GRB but unfortunately they were not possible. The results of the observations were reported in [17].

*GRB 090727:*

This GRB was observed on July 27.9646–28.0063 UT in the  $I$ -band, 0.45–1.45 hours after the gamma-ray event. The afterglow reported by [25] was detected with a magnitude of  $I \sim 19.4$ , using as calibrator the USNO B1.0 star with  $I = 18.72$  and coordinates  $RA_{J2000} = 21:03:49.099$ ,  $DEC_{J2000} = +64:55:58.23$ . The results can be found in [11].

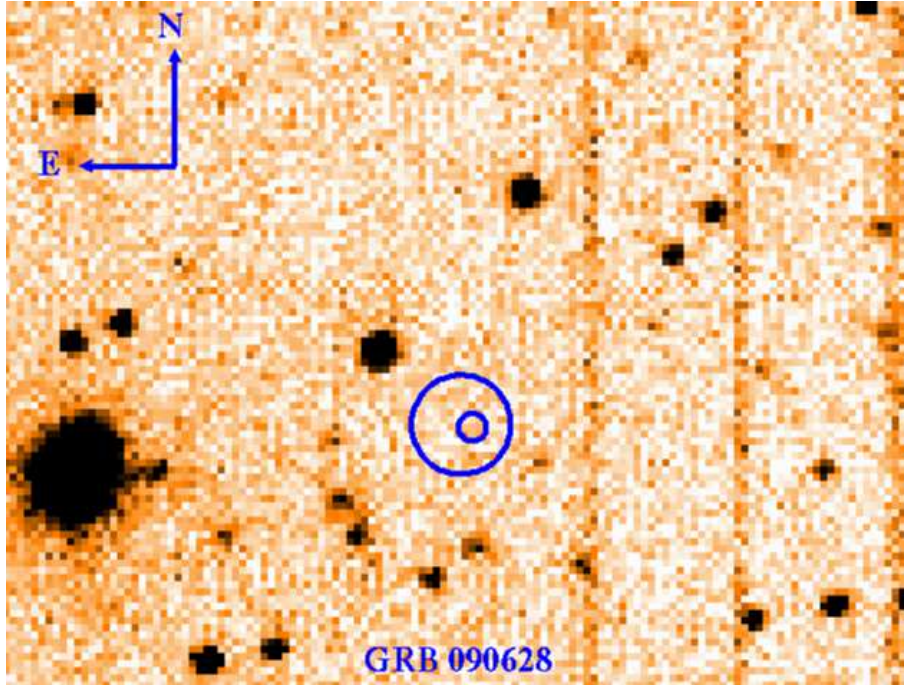


**Fig. 7.** Co-added  $R$ -band image of GRB 090628 taken with the 1.23m telescope. The large circle represents the preliminary XRT error circle [24], whereas the small one shows the refined one [20] reported for GRB 090628. The field of view of the image is  $125'' \times 100''$ . The total exposure time is 3120 s. The individual images were taken on June 28.9486 - 29.0225 UT (1.43 - 3.20 hours after the gamma-ray event). No objects were found in both error circles down to  $R = 22$ . More detailed information can be found in [13].

*The discovery of the optical afterglow of GRB 090813:*

GRB 090813 represents the first optical afterglow discovered with the 1.23m CAHA telescope.  $I$ -band observations of the XRT position were initiated 437s after the GRB trigger, revealing an object with a rough magnitude of  $I \sim 17$  coincident with the XRT position. The lack of the object on the DSS strongly suggested its association with the optical afterglow of GRB 090813. The preliminary results were reported in [12].

*GRB 090814B:*

This is the only GRB detected by the INTEGRAL satellite to date that we have followed up with the 1.23m telescope. We carried out a series of  $I$ -band observations with different exposure times ranging from 180s to 700s. The total exposure time invested for this GRB was 9520s, with a mean observing

epoch of Aug 14.1259 UT. No optical object was found within the refined X-ray error circle provided hours later by XRT. The  $3\sigma$  limiting magnitude of the co-added image is  $I = 20.6$ . A more extended description can be found in [13].

## 4 Conclusions

The 1.23m is a wide-purpose telescope which is currently used by six international teams to perform long-term projects with a duration of four years. The ARAE group of IAA is responsible for automating the telescope operations so that such teams can perform their (usually long) observing campaigns without errors, yet enabling quick override observations of GRBs.

The GRB results obtained to date have been mostly taken by night observers. Use of the fully autonomous mode, provided by RTS2, is pending non-trivial integration of the guider. After this is done, we have reasonable hopes to believe that telescope will be able to react to GRB alerts in a few minutes. This could allow us to detect the optical emission at the first stages of the explosion, making the associated GRB science much more attractive for the GRB community.

We acquired images for seven GRBs, detecting the optical afterglows of four of them. The typical reaction time of these observations ranged from  $\sim 8$  minutes up to a few hours. When fully implemented, the autonomous system should be able to react to triggers within 4 minutes. We have reasonable hopes to obtain much more interesting and world-competitive results in the near future.

### *Acknowledgments*

The research of JG, AJCT, RC and MJ is supported by the Spanish programmes AYA2008-03467/ESP, AYA2009-14000-C03-01 and AYA2007-06377. We are very grateful to all the CAHA staff and in particular to Ulli Thiele for his excellent support with the 1.23m telescope. PK would like to acknowledge generous financial support provided by Spanish *Programa de Ayudas FPI del Ministerio de Ciencia e Innovación (Subprograma FPI-MICINN)* and European *Fondo Social Europeo*. We also would like to thank the two anonymous referees for their helpful comments.

## References

1. S. D. Barthelmy, L. M. Barbier, J. R. Cummings, et al. 2005, *The Burst Alert Telescope (BAT) on the SWIFT Midex Mission*, Space Science Reviews, Vol. 120, 143.
2. D. N. Burrows, J. E. Hill, J. A. Nousek, et al. 2005, *The Swift X-Ray Telescope*, Space Science Reviews, Vol. 120, 165.
3. J.K. Canizzo, S.D. Barthelmy, A.P. Beardmore, et al. 2009, GCN Circ. 9223.
4. S. Castillo-Carrión, & A.J. Castro-Tirado, 2009, *Making preliminary GRBs real-time astronomical reports*, this volume.
5. R. Chornock, W. Li, & A.V. Filipenko, 2009, GCN Circ. 8979.
6. P. A Curren, S.D. Barthelmy, A.P. Beardmore, et al. 2009, GCN Circ. 9545.
7. A. de Ugarte Postigo, et al. 2005, JIBARO: *Un conjunto de utilidades para la reducción y análisis automatizado de imágenes*, in Astrofísica Robótica en España, p. 35. Eds: A. J. Castro-Tirado, B. A. de la Morena, & J. Torres, Madrid.
8. A. Galeev, I. Bikmaev, N. Sakhbullin, et al. 2009, GCN Circ. 9549.
9. J. Gorosabel, P. Kubánek, M. Jelínek, et al. 2009a, GCN Circ. 9236.
10. J. Gorosabel, P. Kubánek, S. Motolla, et al. 2009b, GCN Circ. 9561.
11. J. Gorosabel, N. Huélamo, M. Fernández, et al. 2009c, GCN Circ. 9728.
12. J. Gorosabel, V. Terrón, M. Fernández, et al. 2009d, GCN Circ. 9782.
13. J. Gorosabel, A. de Ugarte Postigo, V. Terrón, et al. 2009e, GCN Circ. 9808.
14. M. Jelínek, A.J. Castro-Tirado, A. de Ugarte Postigo, et al. 2009, *Realtime GRB followup by BOOTES-1B*, this volume.
15. D.A. Kann, S. Klose, B. Zhang, et al. 2007, ApJ in press, [arXiv:0712.2186v2](https://arxiv.org/abs/0712.2186v2).
16. P. Kubánek, et al. 2006, *RTS2: a powerful robotic observatory manager*, Society of Photo-Optical Instrumentation Engineers (SPIE) Conference Series, vol. 6274.
17. P. Kubánek, N. Morales, J.L. Ortiz, et al. 2009, GCN Circ. 9589.
18. P. Kubánek, 2009, *RTS2 – the Remote Telescope System*, this volume.
19. A.J. Levan, P. Curran, K. Wiersema, et al. 2009, GCN Circ. 9547.
20. V. Mangano, B. Sbarufatti, et al. 2009, GCN Circ. 9599.
21. A. Melandri, et al. A&A in preparation.
22. D.G. Monet, S.E. Levine, B. Canzian, et al. 2003, AJ 125, 984.
23. S.F. Sánchez, et al. 2007, PASP, 119, 1186.
24. B. Sbarufatti, V. Mangano, et al. 2009, GCN Circ. 9586.
25. R.J. Smith, C.G. Mundell, et al. 2009, GCN Circ. 9719.